New techniques in ultraviolet astronomical polarimetry: Wide-field imaging and far-ultraviolet spectropolarimetry

K.H. Nordsieck, P. Marcum, K.P. Jaehnig, and D.E. Michalski

Space Astronomy Lab, University of Wisconsin, 1150 University Ave, Madison WI 53706-1390 USA

ABSTRACT

Two sounding rocket payloads under development at the Space Astronomy Laboratory are intended to explore different forms of ultraviolet astronomical polarimetry as a follow-up to the successful mission of the Wisconsin Ultraviolet Photo-Polarimeter Experiment ("WUPPE"). The unknown territory of diffuse-object ultraviolet polarimetry is to be explored by the Wide-Field Imaging Survey Polarimeter ("WISP"). WISP is a quite unusual integrated fast telescope/polarimeter optimized for the wavelengths 135-260 nm. The telescope is a 19.5 cm f/1.9 all-reflective Schmidt; the first element is a large rotatable waveplate constructed of 10 cm panes of CaF_2, which are made birefringent by linear pneumatic actuators along two edges. Preceding the telescope primary is a large Brewster-angle polarizing mirror which makes use of a high-index opaque monolayer. The detector is a UV-sensitized CCD. This instrument will be used to obtain ultraviolet polarimetric images of starlight scattered from diffuse galactic dust clouds over a 1.7×5° field of view with 15 arcsec resolution. The first WISP flight is scheduled for Fall 1993, targeting the Pleiades reflection nebula. Just in its early development is another sounding rocket payload, the Far-Ultraviolet Spectropolarimeter ("FUSP"). This instrument is to have a resolution of better than 0.1 nm and a spectral coverage from 105 to 145 nm. It will consist of a 0.4m parabolic primary with polarimetric optics at the prime focus and a far ultraviolet spectrometer. The polarimetric analyzer will be a thin stressed-LiF waveplate, followed by a diamond Brewster-angle polarizer.

1. INTRODUCTION

Because of the very wide range of astrophysical phenomena, even the subfield of astronomical polarimetry is very broad indeed. In the visible, polarimetric devices span the continuum of spectral resolution (color filters vs Zeeman spectroscopy), spatial resolution (interferometry vs wide-field imaging), and time resolution (millisecond polarimetry of pulsars vs yearly monitoring of variable stars). As a natural extension of the pioneering ultraviolet spectropolarimetry of WUPPE (see earlier paper in this volume), we are exploring the extremes of ultraviolet polarimetric techniques using sounding rocket payloads, guided by what seem to us to be unique advantages of polarimetry in the ultraviolet. The Wide-Field Imaging Survey Polarimeter (WISP) is intended to push to the limit polarimetric sensitivity to faint diffuse light, taking advantage of the very low sky background in the ultraviolet. The field of view is designed to facilitate an all-sky survey in one year from a small satellite like those envisioned in the NASA "SMEX" (SMall EXplorer) program. The Far-Ultraviolet Spectropolarimeter (FUSP) is to extend WUPPE to short wavelengths as far as

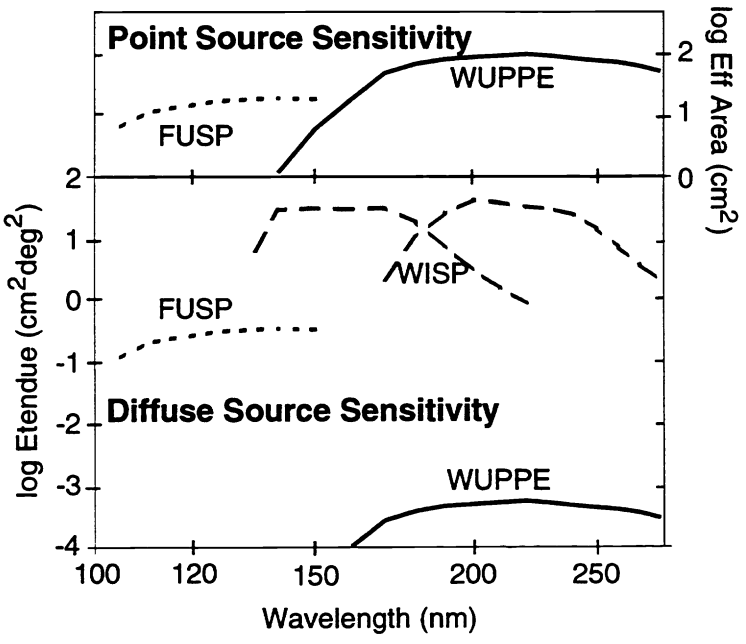

Figure 1. WISP, FUSP, WUPPE Sensitivity

0-8194-1259-7/94/$6.00

is possible with optical polarimetric elements, while increasing spectral resolution sufficiently to take advantage of the large number of astrophysically-important resonance lines in the far UV. WISP is presently being integrated and will be flown for the first time in late 1993; FUSP is in development for a launch in 1996. Figure 1 shows a comparison of the actual and predicted sensitivities of WUPPE, WISP, and FUSP to point and diffuse objects (the latter comparison uses the etendue, the product of the effective aperture and the field of view).

2. WIDE-FIELD IMAGING SURVEY POLARIMETER (WISP)

2.1 Scientific motivation

Diffuse nebulae provide astronomy with one of the most familiar applications of polarimetry: maps of linearly polarized light in comets, reflection nebulae, and the Crab nebula are well-known textbook examples. Yet despite this, physical analysis based on diffuse-object polarimetry is still rare. The primary reason for this is the confusion of processes that greatly complicate measurement and analysis of ground-based visible-wavelength diffuse polarimetry. For instance, the highly polarized variable background of the night sky is a serious obstacle (the polarization of the sky is the other textbook illustration of polarization), and atmospheric transparency changes limit the accuracy of diffuse polarimetry. Beyond these terrestrial problems, one encounters polarized zodiacal light background, unpolarized atomic emission from dilute HII regions, and interfering radiation from ubiquitous foreground and background stars, to name a few. In the ultraviolet all these complications vanish: one is left with a smaller number of hot stars illuminating pure reflection nebulae, a few supernova remnants, the galactic diffuse radiation (itself a reflection nebula), and clear views of external galaxies. Most of these are likely to be polarized, and all are viewed against an extremely dark extragalactic background. It is this realization that motivates the WISP project.

Table 1. WISP observation candidates

Name	Comment
Pleiades	Closest bright RN
NGC 7023	Brightest RN; dust study
N. Amer. Neb	Large RN
M81/82	Foreground DGL; M82 knots
Draco Cloud	DGL; X-Ray shadow
Lockman Win	DGL; Extragalactic background
LMC	Large external galaxy
M31	External galaxy; DGL

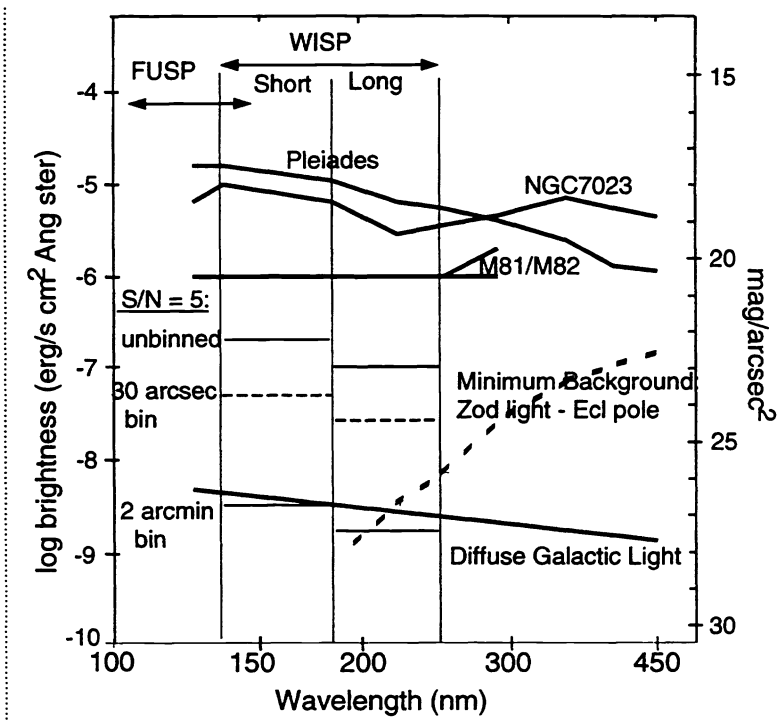

Figure 2. Diffuse UV targets and WISP sensitivity

Table 1 lists several prime observation targets of WISP. These include galactic reflection nebulae (RN), in which individual hot stars illuminate nearby interstellar dust clouds within the field of view. UV polarimetry of the scattered light in RN's will be used to study the UV optical properties of interstellar dust. Second, the Diffuse Galactic Light (DGL) is a pervasive diffuse background in the galaxy in which diffuse clouds are illuminated by distant stars. In the UV a small number of hot stars in clusters provide the illumination; which cluster is the source will be identifiable by polarization position

angle. Polarimetry of the DGL will be used to study the 3-D distribution of galactic dust. Finally, external galaxies are basically diffuse galactic light, viewed from the outside. UV polarimetry will then be used to study the dust properties and 3-D structure of other galaxies. Figure 2 shows the surface brightness of several of these targets, together with the zodiacal light background and the WISP sensitivity for 200 second exposures.

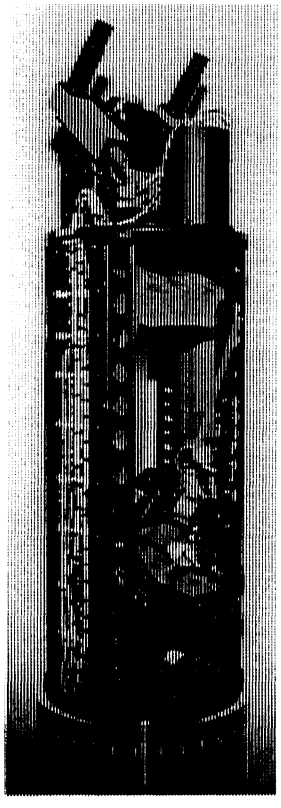

Figure 3. The WISP Payload

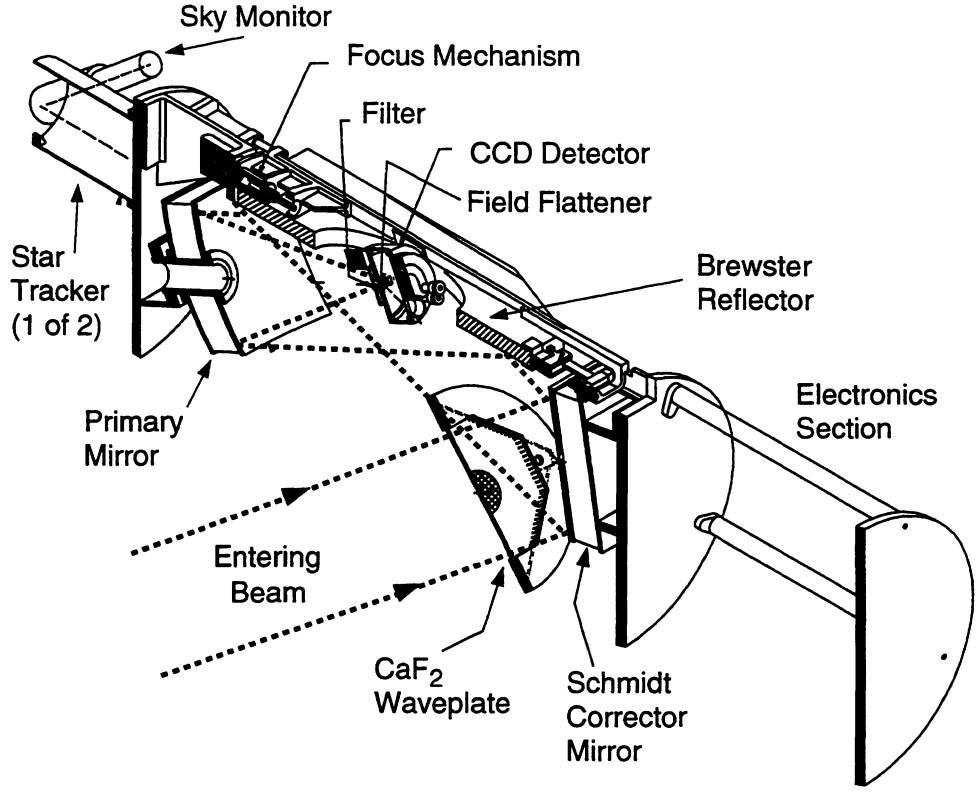

Figure 4. WISP cutaway diagram

2.2 Optical Design

Three technical requirements have governed the development of the WISP payload: First, the experiment is an imaging system optimized for faint diffuse-object studies. Imaging allows the reliable removal of point sources from large-scale nebulosity, and allows resolution of structure within the nebulosity. Second, the major goal of the instrument is a capability for high-accuracy polarimetry. This requires a polarimetric modulation technique capable of removing the effects of throughput and detector sensitivity changes. Third, the instrument is optimized for the vacuum UV, down to 135 nm, just above the atomic Oxygen airglow lines. These requirements lead to an unusual optical design. Candidates for ultraviolet wide-field telescopes are the reflective-corrected Schmidt[1] and Paul-Baker[2,3] designs. Candidates for UV polarizers are one-beam reflective polarizers and one- or two-beam MgF_2 beam-splitters. The polarizer most appropriate for diffuse studies is a one-beam reflective polarizer, since it is free of the chromatic aberration and image overlap problems introduced by beam-splitters. The WISP optical design mates a Brewster-angle polarizer with a fast Schmidt telescope by inserting a fixed polarizing mirror in the collimated beam between the Schmidt corrector mirror and primary. A large-aperture rotatable waveplate which is the first element of the system provides polarimetric modulation without changing the location or polarization state of the image at the detector. In addition, with the modulation device being the first optical element, the instrumental polarization should be very low. The resulting system is roughly 5 orders of magnitude more sensitive to diffuse light than WUPPE (Figure 1).

A diagram and photograph of the WISP payload are shown in Figures 3 and 4. The first optical element is a 19.5 cm aperture ultraviolet waveplate, which is assembled from four flat, square plates of CaF_2, supported by a framework and coupled on two sides to pneumatic actuators. The entire plate may be given any desired phase retardation parallel to its sides at a selected wavelength by changing the force on the actuators. Light enters this element at 40° to the vehicle axis through a deployable door. The next element is the reflective corrector for the Schmidt telescope, which is 30° off-axis. Third, the polarizer, which is a flat mirror tilted at the Brewster angle (67.5°) of an opaque, high-index coating material (currently Y_2O_3). Fourth, a 37.5 cm focal length (f/1.9) primary mirror, giving a focal plane scale for one 27μ pixel of 14.4 arcsec. The primary and corrector have conventional MgF_2 overcoated Aluminum coatings. The detector is in an elliptical hole in the brewster mirror. Just in front of the detector, and serving as the window of the detector housing, is a MgF_2 field-flattener. In front of the field-flattener is a shutter and two thin-film ultraviolet filters on a two-position slide mechanism. Broad-band filters designed for the first flight have central wavelengths of 164 and 218 nm, half-power widths of 47 and 58 nm, respectively, and a visible light leak less than 10^{-4}. The different filter substrates are of different thickness and power to counteract chromatic aberrations in the field flattener. Stray light and other backgrounds are minimized by super-polishing of all optical elements, and baffling; UV zodiacal light and NO atmospheric emission will be monitored in-flight by two photomultipliers with one-inch "sky monitor" telescopes co-pointed with the main telescope.

The above design was optimized using the BEAM4 optical raytrace package. Sample spot diagrams showing on-axis, half-field, and full-field images for two sample filters are shown in Figure 5. The image at the central wavelength of the filter is almost always smaller than one pixel. With the integrated light from the above filters, the total rms spot diameter is still smaller than 17 microns and the full diameter is smaller than about 40 microns (1.5 pixels, 22 arcsec). The telescope mirrors were figured by Lam Optics (Tucson AZ) on HexTek honey-combed blanks. The system agrees with the design to better than 1/6 wave, and the measured rms surface roughness is better than 8 Å. The 55x25 cm rectangular, 3 cm thick, flat Brewster reflector substrate is a lightweighted casting of borosilicate glass, and was polished to better than 15 Å roughness by HekTek Corp.

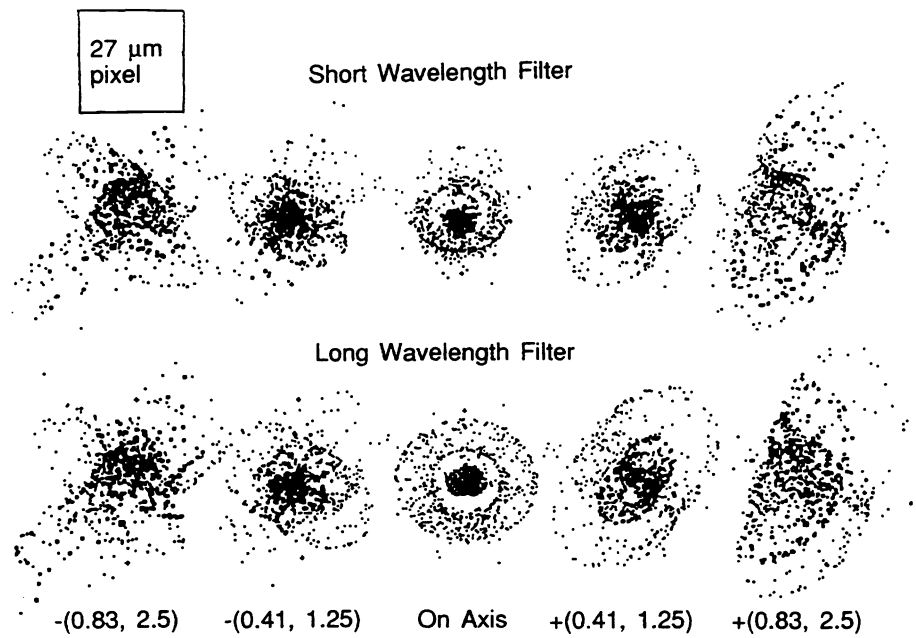

Figure 5. WISP spot diagrams for short, long wavelength filters (large dot: central wavelength; small dot: extreme wavelengths). Field positions are in degrees perpendicular and parallel to the long axis of the detector.

Because of the sensitivity of this very fast telescope to defocus by mechanical and/or thermal changes during launch, an in-flight focus mechanism will allow the detector assembly to be shifted slightly. A small gas discharge mercury lamp and two penta-prisms will project two parallel beams of UV light through the optical train and result in two images of the source on the detector. In a fashion analogous to "split-screen" focus systems in photographic cameras, the processor will utilize sub-array readouts of the detector and centroiding algorithms to control a focus mechanism. The focus mechanism will translate the detector assembly in an iterative fashion until the two images are made collinear.

2.3 Detector/ Electronics

The WISP detector is a phosphor-overcoated, frontside-illuminated Reticon RA1200J CCD, which has 400 X 1200 27μ square pixels. This gives a field of view of 1.7 × 5°. The detector is mounted with its long axis perpendicular to the plane of tilt of the corrector and brewster mirrors (the off-axis imaging is best in this direction). CCD's are the optimal detector for polarimetry because of their inherent stability and high dynamic range, which is necessary to achieve high precision. Very respectable quantum efficiency has already been achieved with simple lumigen phosphor overcoating[4], and substantial improvements may be realized in the near future using thinned chips. The major drawback of CCD's for ultraviolet detection is that they are not solar-blind. However, for the WISP application, high visible-light rejection is not required since the UV diffuse light tends to be blue. For the WISP detector, the nominal system readout noise is projected to be 6 rms electrons. 15 bit digitization is done at a rate of one pixel per 24 microseconds; thus a complete image readout is performed in 12 seconds. The CCD is installed in an evacuated housing and cooled thermoelectrically to -55°C. Heat generated by the thermoelectric cooler is transferred to a copper cold sink reservoir, which is cooled to -45°C before flight by an LN_2 bleedoff refrigerant system.

The electronics section of the experiment, containing power supplies, CCD camera controller, and experiment microprocessor, is in a separate module. The CCD controller is a flight-qualified general purpose controller based on a design by Photometrics, Ltd. The microprocessor, a Motorola 6809, commands the CCD controller, and controls the mechanisms (waveplate rotator, focus, and filter motors, shutter solenoid, and waveplate pneumatic force actuator), science and engineering data flow to the telemetry section, and the overall timeline. Telemetry is through two PCM transmitters, one at a 2 Mbit/second rate which contains real-time raw CCD readout data, and the other at 800 Kbit/second for engineering status. For pointing control of the payload, two standard star-trackers are mounted at the front of the payload, one pointed along the vehicle axis, and the other aligned with the experiment optical axis; this should give ±5 arcsec pointing stability.

Table 2. UV Brewster monolayer candidates

Mat'l	Abs	n(175)
Si_3N_4	180	2.75
Y_2O_3	190	2.7
La_2O_3	195	~2
Nd_2O_3	202	~2
ZrO_2	228	~2
Ta_2O_5	280	>2

2.4 Polarimetric optics

Brewster reflection devices have been used for some time as vacuum UV polarizers. Typical configurations use two or three successive reflections off gold coatings[5] or MgF_2 substrates. These provide high polarization but very low throughput, and the geometry is difficult for large beams. For a single reflection polarizer, a large polarimetric efficiency and throughput may be obtained with a coating material which has a high index of refraction. An additional requirement for ease of calibration is that the material be opaque throughout the ultraviolet in order to suppress interference effects which would likely be non-uniform over a large mirror. Several candidate coating materials, along with the wavelength of the absorption edge and the index at 175 nm, are given in Table 2. Silicon nitride and yttrium oxide are known candidate materials which form stable coatings on glass; in addition, we have been measuring refractive indices of a number of heavy-metal oxides which look promising. Figure 6 illustrates the polarimetric efficiency of several materials for a reflection angle of 67.5 degrees.

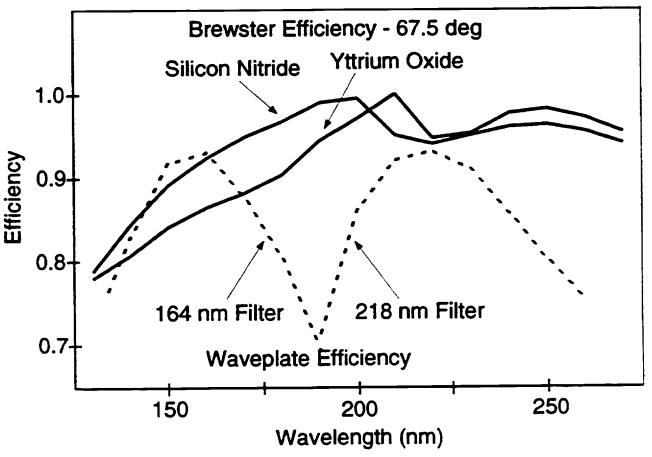

Figure 6. WISP Polarimetric Efficiency.

The design calls for a large aperture retardation

plate to modulate the beam arriving at the polarizer. In the vacuum ultraviolet below 160 nm, there is only one naturally birefringent transparent crystal, magnesium fluoride. The disadvantage of MgF_2 waveplates is that they must be constructed of a sandwich of two opposing waveplates which is very sensitive to angle, difficult to fabricate in large apertures, and ineffective below 140 nm. However, any crystal may be made birefringent by compressing it perpendicular to the direction of the beam. "Piezo-birefringent waveplates" of LiF have been used in the far UV[6] and studies of this phenomenon indicate that CaF_2 has a particularly well-behaved piezo-birefringence down to its cutoff at 130 nm[7]. Large-aperture optical and infrared-wavelength piezo-birefringent waveplates which are modulated rapidly by piezo-electric transducers have been used for many years[8]. In WISP, a large aperture UV waveplate is assembled from four flat, 10 cm square plates of oriented CaF_2 crystal (fabricated and polished by STI/Harshaw, Inc), supported by a framework and coupled on two sides to pneumatic actuators. The entire plate may be given any desired phase retardation parallel to its sides at a selected wavelength simply by changing the force on the actuators. For instance, the force required to achieve half wave retardation at 200 nm for CaF_2 is about 80 lbs/linear inch of edge. The linear polarization Stokes parameters Q,U may be obtained by pairwise combinations of force and rotation to three angular positions. A "Q Stokes image" is formed from two exposures Q+ and Q- by $Q = (Q+ - Q-) / (Q+ + Q-)$, and similarly for U, with the exposures defined as in Table 3. For other wavelengths, the force scales approximately linearly with the wavelength. To obtain a linear polarization map of one field at two wavelengths, eight exposures are then required. By optimizing the force for the central wavelength of a particular filter, the modulation remains above about 70% over the passband. The efficiency shown in Figure 6 includes the effects of the measured nonuniformity of the strain over our waveplate aperture.

Table 3. WISP Waveplate States

Exposure	Phase (200 nm) Ret.	Angle	Force
Q+	0	45	0
Q-	0.5	45	80
U+	0.5	22.5	80
U-	0.5	67.5	80

3. FAR-ULTRAVIOLET SPECTROPOLARIMETER (FUSP)

3.1 Scientific motivation

To the best of our knowledge, useful extra-solar system astronomical polarimetric data in the Far Ultraviolet (91- 145 nm) have never been obtained. Technical obstacles have included design of high-efficiency polarimetric optics, and one important scientific obstacle has been the lack of any UV astronomical polarimetry on which to base experiments. Technical experience in building WUPPE and WISP has now led us to a highly efficient polarimetric modulator/analyzer which works down to 105 nm. Two practical astronomical factors then suggest incorporation of these elements into a spectropolarimeter (rather than low-resolution polarimeter): the ubiquity of strong astrophysical absorption and emission lines in this region, which appear to be important in polarizing stellar envelopes, and the presence of strong airglow and geocoronal lines which must be removed for useful diffuse-object work.

Table 4. FUSP candidate stellar targets

Prog	Target	m_{133}	Δnm	ΔP_{req}	ΔP_{pred}	Comment
Be	γ Cas	-1.6	0.1	.1%	.05%	No shell lines
	ζ Tau	-0.33	0.1	.1	.08%	Shell, WUPPE obs
	PPCar	0.43	0.1	.1	.13	Shell, WUPPE obs
WR	γ Vel	-2.6	0.3	.05	.02	WC8 + O
	EZCMa	2.5	0.3	.2	.18	WN5, WUPPE obs
SG	β Ori	-0.8	0.1	.05	.06	
ISM	σ Sco	-0.48	3	.05	.015	λ_m=560 nm
	α Cam	1.95	3	.1	.05	λ_m=500,WUPPE,pol SG
	ρ Oph	2.05	3	.05	.05	λ_m=680 nm
	κ Cas	2.7	3	.1	.06	λ_m=530,WUPPE,pol SG

Table 4 lists several candidate stellar targets together with the 133 nm magnitude, the required resolution and precision, and the predicted FUSP precision for a 300 second exposure. The Be star program is an extension of results from WUPPE[9] in which the polarization from electron scattering in the disks of these rapidly-rotating stars was found to be unexpectedly modified by competing weak FeII resonance absorption

lines. Far UV spectropolarimetry would allow us to study the polarimetric effects across the very strong far UV resonance lines that are seen in the spectra of these stars. Wolf-Rayet (WR) stars are stars in an advanced stage of evolution which possess very wide, strong resonance emission lines from dense stellar winds. The WUPPE results from one of these stars, EZ CMa[10] exhibits large polarization effects that conflict strongly with similar effects seen in the visible. Blue supergiants (SG) exhibit weak polarimetric line effects in the visible; very strong far UV emission/absorption resonance lines should allow for dissection of the geometrically complex envelopes of these stars. Finally, a natural extension of the WUPPE studies of polarization by the interstellar medium (ISM)[11] is required to interpret intrinsic polarization in the far UV. Some models predict strong changes in the interstellar polarization in this region due to rapid changes in the optical properties of interstellar dust grains. The varied environment of these dust grains is indicated by the different wavelengths of maximum polarization (λ_m) toward these stars. Possible diffuse-light studies by FUSP include a far UV follow-up of WISP results for the brighter reflection nebulae.

3.2 Instrument Overview

Figure 7 illustrates the design concept for the FUSP optical section. The telescope is a simple 40 cm F/3 parabola: the aperture is the largest that will fit in a 17-inch rocket skin, and the f-ratio is the fastest that may be accommodated by the spectropolarimeter. At the prime focus is mounted the spectropolarimeter, an evacuated housing with the polarimetric elements near the focus. Evacuation is desirable because close clearances of the detector in the spectrometer preclude a separate detector vacuum housing, and because this would allow much better control of contamination of the detector and spectrometer optics coatings. The primary mirror and spectrometer coatings will probably be LiF-overcoated Aluminum. The spectrometer design shown here is a fast, imaging system using a blazed plane grating for maximum throughput. Imaging allows for accurate removal of scattered light for stellar work, and for long-slit imaging of reflection nebulae. Since this is a single-beam polarimeter, much care has been taken to avoid vignetting of the beam in the spectrometer which would result in photometric changes with pointing. An on-axis, nearly parabolic collimator illuminates a perforated 100 mm 2400 groove/mm plane grating. A f/3.75 spherical Schmidt mirror focusses the dispersed beam through the grating perforation so that the detector does not vignette the beam. The grating perforation is in turn hidden behind the obscuration by the spectrometer of the beam from the sky. An asphere on the collimator compensates for spherical aberration in the Schmidt camera. The spectrometer focal-plane scale is 138 arcsec/mm, so that ±5 arcsec pointing stability leads to 70 micron (2.5 pixel) image blur. The other main source of image blur is uncompensated field curvature; an image rms diameter better than three pixels (0.1 nm, 10 arcsec) along the dispersion and 25 arcsec perpendicular to the dispersion is obtained. We plan to use a UV sensitized CCD similar to the WISP detector: it has the same advantages for polarimetry of large dynamic range and stability, and would allow use of a duplicate WISP electronics section for FUSP. The 400×1200 pixel format of the Reticon CCD provides a wavelength coverage from 105-145 nm and a slit length greater than 20 arcmin.

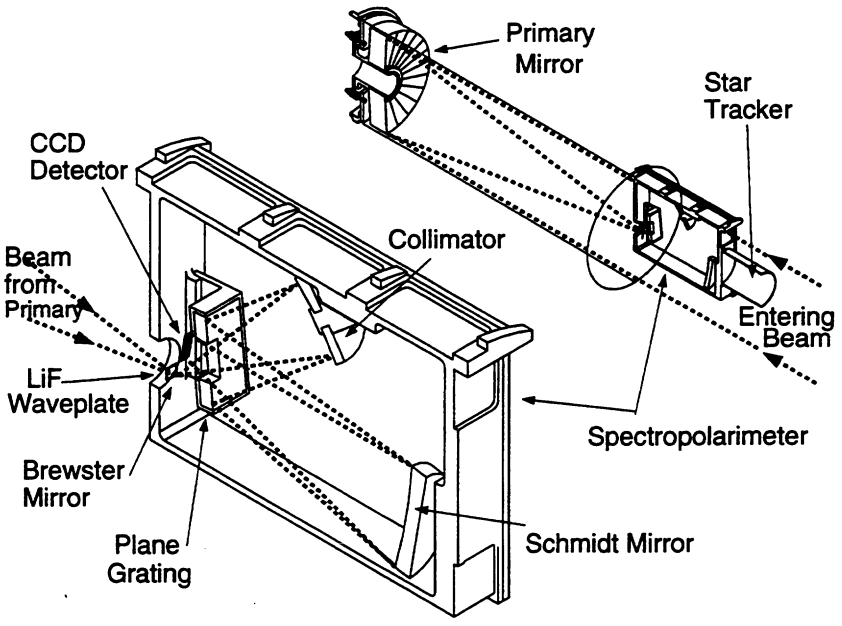

Figure 7. FUSP Optical Design. Left: blowup of spectropolarimeter.

3.3 Polarimetric Optics

The polarimetric optics of FUSP is basically an extrapolation of the techniques of WUPPE (waveplate modulator/ analyzer at the entrance to a spectrometer) and WISP (piezo-birefringent waveplate, Brewster reflection analyzer) to the lowest possible wavelengths.

The polarimetric modulator is a 1cm square, 1mm thick stressed-LiF waveplate, mounted just before the focus. The waveplate is made to be halfwave at 124 nm by applying about 15 pounds pressure to one edge of the plate; polarimetric modulation is performed by rotating the plate 45°, which rotates the plane of polarization by 90°. The LiF plate is the only transmissive element in the instrument, and results in a short-wavelength limit of 105 nm. The piezo-birefringence of LiF has been measured down to 120 nm by Sanchez and Cardona[7]; it increases rapidly as one approaches the UV absorption edge at 105 nm, which limits the useful simultaneous bandwidth to less than 50 nm. It will be necessary to undertake laboratory measurements of the piezo-birefringence at lower wavelengths to better quantify the optimal spectral coverage. The estimated linear polarimetric efficiency of a LiF waveplate, using extrapolated piezo-birefringence, is shown in Figure 8. A fixed pressure on the LiF plate will be applied by a mechanical collet. A strain gauge mounted to the LiF plate will monitor any changes in the strain with time or temperature for post-flight calibration purposes. The LiF plate will be the entrance window to the evacuated spectrometer.

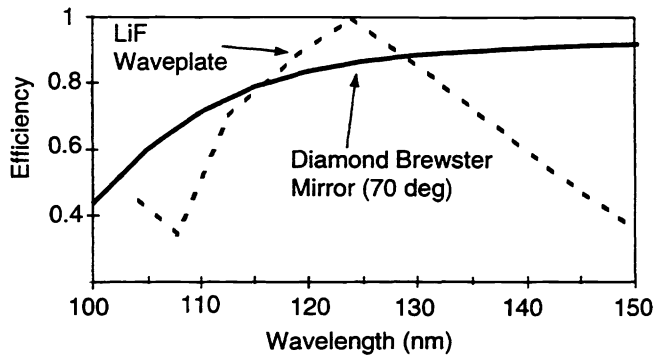

Figure 8. FUSP analyzer and modulator efficiency

The polarization analyzer is a very small diamond mirror mounted at the telescope prime focus at an angle of incidence of 70°. The materials requirement for Brewster reflection is an index of refraction greater than 1; the greater the index of refraction, the higher the Brewster angle, and the higher the reflectivity at the Brewster angle. Diamond is the only known material to maintain its index greater than 1.5 down to 105 nm: in fact it remains above 3 for the entire FUSP range. Small, very thin natural diamond windows are available in the appropriate sizes. Because diamond is opaque below 170 nm, only the first surface, not internal defects, are important. A calculation of the polarization efficiency of a diamond mirror in an F/3 beam at 70° incidence is shown in Figure 8.

In operation, the FUSP experiment timeline would consist of fairly short exposures, approximately 10 seconds, on each waveplate position. The CCD readouts would be binned roughly 2x4 pixels to reduce the readout time to less than 1 second. For half of the total dwell on a target, the filter would toggle between an angle of 0 and 45° (giving the Q+ and Q- images, see section 2.4) and the other half on ±22.5° (U+ and U-). This should give the highest possible precision achievable with a one-beam device, better than 0.1%. The estimated effective area and etendue (cm^2deg^2) is shown in Figure 1. We assume mirror efficiencies of 80%, obscuration 20%, brewster reflectivity 35%, grating efficiency 50%, actual LiF transmission, and detector quantum efficiency 20%. A 300 second exposure on a 0^m (flat F_λ) object will give $\equiv 10^6$ photons/resolution element (0.1% polarimetric precision) at 120 nm.

4. ACKNOWLEDGEMENTS

WISP and FUSP are supported by NASA grant NAG5-647.

5. REFERENCES

1. D.J. Schroeder, "All-reflecting Baker-Schmidt flat-field telescopes," *Applied Optics* **17**, pp. 141-144, 1978.

2. J.G. Baker, "On improving the effectiveness of large telescopes," *IEEE Aerospace* **AES-5**, pp. 261-272, 1969.

3. J.T. McGraw, H.S. Stockman, J.R.P. Angel, H. Epps, and J.Y. Williams, "Charge-coupled device (CCD)/transit instrument (CTI) deep photometric and polarimetric survey - a progress report," *SPIE* **331** Instrumentation in Astronomy pp. 137-150, 1982.

4. P.F. Morrissey, S.R. McCandliss, P.D. Feldman, and S. Friedman, S., "Ultraviolet performance of a Lumigen-coated CCD," (Abstract) *Bulletin American Astronomical Society* **23**, p. 1316, 1992.

5. V.G. Horton, E.T. Arakawa, R.N. Hanine, and M.W. Williams, "A triple reflection polarizer for use in the vacuum ultraviolet," *Applied Optics* **8** pp. 667-670, 1969.

6. H. Metcalf, and J.C. Baird, "Circular polarization of vacuum ultraviolet light by piezobirefringence," *Applied Optics* **5**, pp. 1407-1410, 1966.

7. C. Sanchez, and M. Cardona, "Piezobirefringence in the vacuum ultraviolet: alkali halides and alkaline-earth fluorides," *Phys. Stat. Sol. (b)* **50**, pp. 293-304, 1972.

8. J.C. Kemp and M.S. Barbour, "A photoelastic-modulator polarimeter at Pine Mountain Observatory," *Pub. Astronomical Society of the Pacific* **93**, pp. 521-525, 1981.

9. K.S. Bjorkman, K.H. Nordsieck, A.D. Code, C.M. Anderson, B.L. Babler, G.C. Clayton, A.M. Magalhães, M.R. Meade, M.A. Nook, R.E. Schulte-Ladbeck, M. Taylor, and B.A. Whitney, "First spectropolarimetry of Be stars from the Wisconsin Ultraviolet Photo-Polarimeter Experiment," *Astrophysical Journal* **383**, pp. L67-L70, 1991.

10. R.E. Schulte-Ladbeck, K.H. Nordsieck, A.D. Code, C.M. Anderson, B.L. Babler, K.S. Bjorkman, G.C. Clayton, A.M. Magalhães, M.R. Meade, D. Shepherd, M. Taylor, and B.A. Whitney, "The first linear polarization spectra of Wolf-Rayet stars in the ultraviolet: EZ Canis Majoris and θ Muscae," *Astrophysical Journal* **391**, pp. L37-L40, 1992.

11. G.C. Clayton, C.M. Anderson, A.M. Magalhães, A.D. Code, K.H. Nordsieck, M.R. Meade, M.J. Wolff, B. Babler, K.S. Bjorkman, R.E. Schulte-Ladbeck, M.J. Taylor, and B.A. Whitney, "The first spectro-polarimetric study of the wavelength dependence of interstellar polarization in the ultraviolet," *Astrophysical Journal*, **385**, pp. L53-L57, 1992.